High-twist production of prompt single photons at large transverse momentum

Edmond L. Berger
High Energy Physics Division, Argonne National Laboratory, Argonne, Illinois 60439
(Received 14 December 1981)

Quantitative predictions are presented for a specific hard-scattering reaction $\pi N \to \gamma X$ in which both the incident meson and the produced prompt photon couple directly in the QCD amplitude. The process leads to a highly constrained class of events at large p_T in which the photon momentum is balanced by that of a recoil quark jet, with no spectator jet of final-state particles emerging along the beam axis. Normalized absolutely in terms of the electromagnetic form factor of the pion, $F_\pi(Q^2)$, the cross section provides a lower bound on the total $p_T{}^{-6}$ high-twist contribution to the inclusive prompt photon yield.

I. INTRODUCTION

It has been observed for some years that the production of hadrons, prompt photons, and hadron jets at large transverse momentum is not described by the simple $p_T{}^{-4}$ dependence predicted by the leading-twist quantum-chromodynamics (QCD) amplitudes. Gluonic radiative corrections steepen the p_T dependence, as would be desirable for agreement with data. However, recent analyses of the high-energy data from inclusive deep-inelastic lepton scattering[1] show that these radiative corrections are relatively modest, characterized by a scale $\Lambda \simeq 100$ MeV. Thus, there is new motivation for trying to estimate the size and other physical properties of high-twist $p_T{}^{-6}$ and $p_T{}^{-8}$ QCD contributions to the inclusive yield at large p_T. Important high-twist contributions have been inferred from analyses of data from some inclusive hard-scattering processes, but the evidence is not unambiguous. The data from deep-inelastic lepton scattering show that a substantial fraction of the Q^2 dependence at modest values of Q^2 ($\lesssim 20$ GeV^2) may be attributed to high-twist terms in the structure functions.[1] This evidence of inverse power dependence complements that obtained elsewhere. In the Drell-Yan process $\pi N \to \gamma^* X$, the high-twist term is observed as a dominant longitudinal polarization[2,3] of the γ^* as the longitudinal-momentum fraction $x_F \to 1$. Likewise, in $\nu N \to \mu^- \pi^+ X$, an important $(1-y)$ component[4,5] of $d\sigma/dy$ is identified for large values of $z_\pi = E_\pi/\nu = p_\pi \cdot p_N / Q \cdot p_N$.

In this paper, a specific high-twist coupling of the incident meson in meson-nucleon collisions is shown to lead to a special class of prompt photon events at high transverse momentum. In these events, no final-state spectator jet emerges along the beam direction, and the kinematics are highly constrained such that the longitudinal and transverse momentum of the recoil quark jet are specified uniquely by those of the observed prompt photon. The high-twist QCD process in question is sketched in Fig. 1(a). It may be contrasted with conventional leading-twist QCD scattering, illustrated in Fig. 1(b), in which the prompt photon is produced along with a recoil jet, as well as spectator jets along both the beam and target axis directions. The cross section for the particular class of high-twist events discussed here, predicted absolutely in terms of the pion's electromagnetic form factor $F_\pi(Q^2)$, provides a lower bound on the total $p_T{}^{-6}$ high-twist contribution to prompt single-photon production. Thus, identification of this signal is important for establishing experimental bounds on the full $p_T{}^{-6}$ contribution to $E\,d\sigma/d^3p_\gamma$. Experiments with high-intensity $\pi^\pm$ beams in the laboratory momentum range of 200 to 400 GeV/c would seem to be especially ap-

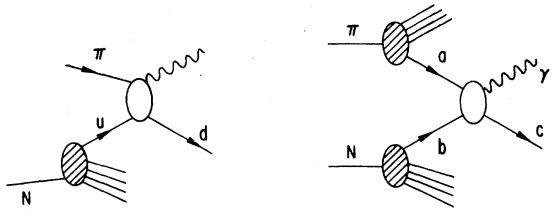

FIG. 1. (a) Illustration of $\pi N \to \gamma d X$ via the QCD high-twist subprocess $\pi u \to \gamma d$. Th unshaded oval represents the full QCD hard-scattering amplitude for $\pi u \to \gamma d$. (b) Illustration of $\pi N \to \gamma c X$ via the QCD subprocess $ab \to \gamma c$, where a and b are constituents of the π and N, respectively.

propriate.

In a previous paper,[6,7] a similarly constrained special class of high-twist purely hadronic jet events was discussed in which, for example, a gluon, g, replaces the prompt photon in Fig. 1. Important differences between the results of the two calculations are associated with the different couplings of the γ and gluon to the quark constituents of the incident meson. In contrast with many simple QCD processes, the high-twist cross sections for $\pi^- q \to \gamma q$ and $\pi^- q \to g q$ are not related by a simple ratio of coupling strengths ($\alpha_{\rm EM}/\alpha_s$). Therefore, the high-twist processes $\pi^{\pm} N \to \gamma X$ permit a new and interesting probe of the electric charges of the constituents of the pion. Prompt photon production is also simpler in two ways: there is only one high-twist Born diagram, and there are no ambiguities in the definition of the final-state trigger jet (γ vs g).

II. HIGH-TWIST AMPLITUDE

The two-body high-twist subprocess studied explicitly here is $\pi q_N \to \gamma q$, where q_N is a constituent of the initial nucleon target. No two-body prompt photon process may be initiated from the gluon distribution in the target, and $\pi \bar{q}_N \to \gamma \bar{q}$ is ignored because the density of antiquarks [$\bar{q}_N(x)$] in the nucleon target is insignificant in the region of relatively large x which contributes to production at large p_T. The only contributions considered are those from the minimal $|q\bar{q}\rangle$ Fock state of the incident pion. Contributions from higher Fock states such as $|q\bar{q}g\rangle$ and $|q\bar{q}q\bar{q}\rangle$ provide more complex final states, including beam jets. Thus, the class of events emphasized in this paper probes the *joint probability* (high twist) for finding both a q and a $\bar{q}$ in the beam, and only a q and a $\bar{q}$.

Continuing to use a procedure[6,8] which has become somewhat familiar, we factor the high-twist amplitude $M(\pi q_N \to \gamma q)$ into two parts: (a) a nonperturbative, process-independent distribution amplitude, $\phi(z,Q)$—the probability amplitude that the valence q and $\bar{q}$ in the pion carry fractions z_1 and $z_2 (z_1+z_2=1)$ of the pion's momentum, and are collinear up to transverse momenta $k_{\perp i} \sim Q$, where Q is the typical momentum transfer in the subprocess; and (b) the hard-scattering amplitude T_H for the subprocess $q\bar{q}+q_N \to \gamma+q$, where the incident q and $\bar{q}$ are collinear with the initial pion; T_H is derived from QCD perturbation theory.

The invariant amplitude for $\pi q_N \to \gamma q$ is obtained as a convolution,

$$M(\hat{s},\hat{t}) = \int_0^1 dz_1 \int_0^1 dz_2 \phi_\pi(z_i,Q)\delta(1-z_1-z_2) T_H(\hat{s},\hat{t};z_i) \ . \tag{1}$$

All of the effects of hadronic binding are contained in the distribution amplitude ϕ_π. The external lines in T_H can be taken as massless if power-law corrections in $1/Q$ are neglected. Sketched in Fig. 2 are the four QCD Feynman-Born diagrams which contribute to $\pi q_N \to \gamma q$, to leading order in $\alpha_s(Q^2)$. They are identical in form to the gauge-invariant set for $\pi q_N \to g q$ studied in Ref. 6, except for the absence of a fifth graph, present in $\pi q_N \to g q$, in which the final gluon couples to the internal exchanged gluon (three gluon coupling). Ignored here are QCD radiative corrections associated with the q_N line which lead to the standard Q^2 evolution for the quark structure function.

Specific labeling of momenta for the T_H Born diagrams is shown in Fig. 2(a). The pion mass is neglected; $m_\pi = 0$. The quark and antiquark constituents of the pion are constrained to form a pseudoscalar, color-singlet state. All amplitudes represented in Fig. 2 carry the same color factor $4\delta_{ij}/(3\sqrt{3})$, where i and j label the color indices of the final and initial quarks in $\pi q \to \gamma q$. The subprocess invariants are $\hat{s}=(p_1+p_\gamma)^2=(p_2+p_\pi)^2$; $\hat{t}=(p_\gamma-p_\pi)^2$, and $\hat{u}=(p_1-p_\pi)^2$. In Figs. 2(a) and 2(b), the exchanged gluon carries the squared-four-momentum $z_2\hat{s}$, whereas in Figs. 2(c) and 2(d), the gluon carries $z_1\hat{u}$. Therefore, in the large-p_T kinematic region of interest these are far-off-shell "hard" gluons.

The diagrams in Fig. 2 separate into two sets: (a) and (b) form one gauge-invariant pair; (c) and (d) form a second. The correct choice of the relative sign between the amplitudes for the two sets may be verified by comparison of the diagrams (a) and (c). This is important because some of the effects to be discussed are based on interference between the two sets. In Fig. 2(a), e_1 and e_2 label the quark (not antiquark) electric charges; in the case of $\pi^- u_N \to \gamma d$, $e_1 = -\frac{1}{3}$ and $e_2 = \frac{2}{3}$.

After deriving explicit Feynman amplitudes for the graphs in Fig. 2, and simplifying the result, I obtain

$$T_H(\pi q_N \to \gamma q) = \frac{4ieg^2\delta_{ij}}{3\sqrt{6}} \frac{1}{z_1 z_2 \hat{s}\hat{t}\hat{u}} \tilde{M}^\mu \epsilon_\mu \ , \tag{2}$$

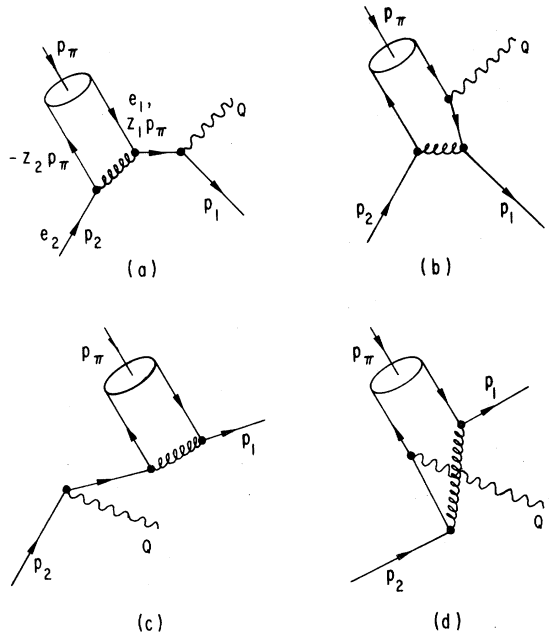

FIG. 2. Full set of QCD Feynman graphs for $\pi+q(p_2)\to\gamma(p_\gamma)+q(p_1)$; in (a), four-vector momenta are denoted by p_π, p_2, Q, and p_1, whereas e_1 and e_2 label quark charges.

with

$$\tilde{M}^\mu=\bar{u}(p_1)\gamma_5(A\gamma^\mu+B^\mu\not{p}_\pi)u(p_2)\ . \tag{3}$$

The functions A and B are expressed as

$$A=-(\hat{s}-\hat{u})(e_2\hat{s}+e_1\hat{u})\ , \tag{4}$$

$$B^\mu=4e_1\hat{u}\,p_1^\mu+4e_2\hat{s}\,p_2^\mu+2(e_2\hat{s}-e_1\hat{u})p_\pi^\mu\ . \tag{5}$$

The symmetry of the distribution amplitude $\phi_\pi(z_i)$ under interchange of z_1 and z_2 permits retention in Eqs. (4) and (5) of only those terms symmetric in the z_i. One may check that $p_\gamma\cdot B=-A$, and, therefore, that $p_\gamma^\mu\tilde{M}^\mu=0$, as is required by gauge invariance. If $e_1=e_2$, the expressions for A and B^μ in Eqs. (4) and (5) become directly proportional to those for the purely hadronic case $\pi q\to gq$ studied in Ref. 6. However, when $e_1\neq e_2$, as is true for $\pi^\pm q\to\gamma q$, the proportionality is broken.

The form of Eqs. (1) and (2) may be compared with the form factor of the pion[8] at large Q^2:

$$F_\pi(Q^2)=\int\int dx_i\delta(1-x_1-x_2)\int\int dy_i\delta(1-y_1-y_2)\phi^*(x_i,Q)\phi(y_i,Q)\frac{16\pi\alpha_s(Q^2)}{3Q^2x_1x_2y_1y_2}\ . \tag{6}$$

Here, as usual, $\alpha_s=g^2/4\pi$. The distribution amplitude $\phi(z_i,Q)$ enters Eqs. (1) and (2) and Eq. (6) with the same weight factor $(1/z_1z_2)$. This implies that the cross section for $\pi q_N\to\gamma q$ may be normalized absolutely in terms of data on $F_\pi(Q^2)$, entirely independently of assumptions about the specific functional form of $\phi(z_i,Q)$.

III. CROSS SECTIONS

For $\pi q_N\to\gamma q$, the absolute square of $M(\hat{s},\hat{t})$, summed over final spins and colors, and averaged over initial spins and colors is

$$\frac{1}{6}\sum_{\substack{\text{colors,}\\ \text{spins}}}|M(\hat{s},\hat{t})|^2=\tfrac{16}{27}e^2g^4\left[\frac{1}{\hat{u}^2}+\frac{1}{\hat{s}^2}\right]\frac{(e_2\hat{s}+e_1\hat{u})^2}{-\hat{t}}\left|\int_0^1\frac{\phi_\pi(z,Q)dz}{z(1-z)}\right|^2\ . \tag{7}$$

The differential cross section for $\pi q_N\to\gamma q$ is then

$$\frac{1}{\pi}\frac{d\sigma}{d\hat{t}}=\tfrac{4}{9}\alpha_{\rm EM}\alpha_s F_\pi(\hat{s})\left[\frac{1}{\hat{u}^2}+\frac{1}{\hat{s}^2}\right]\frac{(e_2\hat{s}+e_1\hat{u})^2}{-\hat{t}\hat{s}}\ , \tag{8}$$

where $\alpha_{\rm EM}\simeq\frac{1}{137}$, and Eq. (6) has been used to eliminate ϕ_π. Equation (8) is correct to leading order in the strong coupling strength $\alpha_s(\hat{s})$. As in Ref. 6, because $d\sigma/d\hat{t}(\pi q_N\to\gamma q)$ has been related to the observed $F_\pi(\hat{s})$, Eq. (8) should include all of the anomalous-dimension $(\ln Q^2/\Lambda^2)^{-\gamma_n}$ contributions from the evolution of the meson distribution amplitude $\phi(z,Q)$. The value of $F_\pi(Q^2)$ is measured[9] for $Q^2\lesssim 4$ GeV^2. For the larger values of Q^2, it may be parametrized as

$$F_\pi(Q^2)=0.4\ \text{GeV}^2/Q^2,\quad Q^2>2\ \text{GeV}^2\ ,$$

and this analytic expression is used to obtain the numerical predictions presented later in this paper.

The cross section for the high-twist (HT) photoproduction process $\gamma q\to\pi q$ is identical to that for $\pi q\to\gamma q$, Eq. (8), except for a different spin-average factor[7]:

$$\frac{1}{\pi}\frac{d\sigma}{d\hat{t}}(\pi q\to\gamma q)=2\frac{1}{\pi}\frac{d\sigma}{d\hat{t}}(\gamma q\to\pi q)\ . \tag{9}$$

The reaction $q_\pi\bar{q}_N\to\pi\gamma$ is another high-twist subprocess which involves pointlike direct couplings of both the π and the γ. Its cross section may be obtained from Eq. (7) upon crossing $\hat{s}\leftrightarrow\hat{t}$ and dividing by a second color- and spin-average factor of 6. Explicit results are presented in the Appendix.

Because all the gluon and photon couplings in Fig. 2 conserve quark helicity, the final quark in $\pi q\to\gamma q$ emerges with the same helicity as the incident quark. Thus the amplitude and the cross section for $\pi q\to\gamma q$ should vanish as $\hat{t}\to 0$. However, this property is not manifested by Eq. (8), which has a pole at $\hat{t}=0$. The conflict is resolved readily if finite quark masses are retained in the calculation. In this case, the factor $\hat{t}^{-1}$ in Eq. (8) is replaced by $\hat{t}(\hat{t}-m_q^2)^{-2}$, and the cross section vanishes, as expected, as $t\to 0$. When $e_1=e_2$ in Eq. (8), the factor $(e_2\hat{s}+e_1\hat{u})^2\to e_1^2\hat{t}^2$ and the cross section shows an additional suppression $\propto\hat{t}^2$ as $\hat{t}\to 0$. The same suppression is true for the purely hadronic reaction $\pi q\to gq$ studied in Ref. 6, but was attributed incorrectly there to helicity conservation. The ratio of the differential cross sections for $\pi q\to\gamma q$ and $\pi q\to gq$ is

$$\frac{\hat{\sigma}(\pi q\to\gamma q)}{\hat{\sigma}(\pi q\to gq)}=\frac{3\alpha_{\rm EM}}{4\alpha_s}\frac{(e_2\hat{s}+e_1\hat{u})^2}{\hat{t}^2}\ . \tag{10}$$

Equation (10) indicates that high-twist production of prompt photons is significantly enhanced over that for gluon-jet production at forward angles.

The inclusive yield of prompt photons in $\pi N\to\gamma X$ is obtained upon multiplying Eq. (8) by the appropriate quark distribution function. For $\pi^- p\to\gamma qX$, this yields

$$\frac{E\,d\sigma}{d^3p_\gamma}=xu_p(x)\left[\frac{s}{s+u}\right]\frac{1}{\pi}\frac{d\sigma}{d\hat{t}}(\pi q_N\to\gamma q)\ , \tag{11}$$

where $u_p(x)$ is the probability that an up quark in the proton carries momentum fraction $x=\hat{s}/s$.

There is no integral to evaluate in Eq. (11); at fixed $s=(p_\pi+p_N)^2$, the values of $\hat{u}$, $\hat{t}$, and x are specified uniquely by the photon momentum p_γ; $u=(p_\gamma-p_N)^2=\hat{u}/x$, $t=\hat{t}$, and $x=-t/(s+u)$.

Equation (11) may be rewritten in the form

$$\frac{E\,d\sigma}{d^3p_\gamma}=\frac{1}{p_T{}^6}f_{\rm HT}(x_T,x_F)\ , \tag{12}$$

where $x_T=2p_T/\sqrt{s}$, and $x_F=2p_L/\sqrt{s}$. The $p_T{}^{-6}$ behavior arises because Eq. (8) is proportional to $\hat{s}^{-3}$ at fixed values of $\hat{u}/\hat{s}$ and $\hat{t}/\hat{s}$. In the limit $x_T\to 1$, a simple analytic expression may be obtained at $x_F=0$ for the x_T dependence of the scaling function $f_{\rm HT}(x_T,x_F)$. In particular, Eqs. (8) and (11) yield $f_{\rm HT}(x_T)\propto u_p(x_T)$ as $x_T\to 1$. Adopting the simple distribution function[10] $xu_p(x)=(1-x)^3$, one derives

$$f_{\rm HT}(x_T)\propto(1-x_T)^3\ , \tag{13}$$

as $x_T\to 1$.

The p_T and x_T dependences of Eqs. (12) and (13) may be contrasted with those characteristic of the leading-twist process sketched in Fig. 1(b). Although the leading-twist (LT) terms provide a $p_T{}^{-4}$ behavior in p_T, the associated scaling function $f_{\rm LT}(x_T)$ falls off more rapidly than Eq. (13). For example, in $\pi^- p\to\gamma X$, the dominant leading-twist subprocess at large x_T is $\bar{u}_\pi u_p\to\gamma g$. If $x_1\bar{u}_\pi(x_1)\propto(1-x)^{n_\pi}$ and $x_2u_p(x_2)\propto(1-x_2)^3$, one obtains

$$f_{\rm LT}(x_T)\propto(1-x_T)^{n_\pi+4} \tag{14}$$

at $x_F=0$. Experimentally[11] it is observed that $n_\pi\geq 1$. Therefore,

$$\frac{\sigma_{\rm HT}(p_T,x_T)}{\sigma_{\rm LT}(p_T,x_T)}\propto\frac{1}{p_T{}^2(1-x_T)^{n_\pi+1}}\ . \tag{15}$$

For any given value of s, the high-twist term will dominate at large enough x_T. Numerical predictions are presented below in Sec. IV.

The dependence of the high-twist cross section on the charge of the incident pion beam is another characteristic difference. Returning to Eq. (8), one observes that

$$\frac{\hat{\sigma}(\pi^- u\to\gamma d)}{\hat{\sigma}(\pi^+ d\to\gamma u)}=\frac{4(1-\frac{1}{2}u/s)^2}{(1-2u/s)^2}\ . \tag{16a}$$

In Eq. (16a), the subprocess invariants $\hat{u}$ and $\hat{s}$ have been eliminated through the substitution $(\hat{u}/\hat{s})=(u/s)$. Recognizing that $(u/s)=-\frac{1}{2}x_R(1+\cos\theta^*)$, where θ^* is the center-of-mass (c.m.)

production angle of the photon, and $x_R = 2p_\gamma^{\text{c.m.}}/\sqrt{s}$, one may rewrite Eq. (16a) as

$$\frac{\hat{\sigma}(\pi^- u)}{\hat{\sigma}(\pi^+ d)} = \frac{4[1+\frac{1}{4}x_R(1+\cos\theta^*)]^2}{[1+x_R(1+\cos\theta^*)]^2} . \tag{16b}$$

This ratio is greater than unity throughout the range $0 \le x_R \le 1$, but it is a decreasing function of x_R. At large x_R ($x_R \to 1$) and $\theta^* = 90°$ ($x_F = 0$), it approaches $\frac{25}{16}$.

The high-twist process considered in this paper specifies that the inclusive yield of prompt photons produced at $x_F = 0$ from an $I = 0$ target (e.g., deuterium or carbon) should be greater for π^- beams than for π^+ beams by a factor which decreases towards $\frac{25}{16}$ as $x_T \to 1$. The leading-twist process $\bar{q}_\pi q_N \to \gamma g$ favors production by π^- beams on $I = 0$ targets by a healthy factor of $(e_u/e_d)^2 = 4$. This difference between the charge dependence of the leading-twist and high-twist contributions has important implications for attempts to isolate the leading-twist annihilation subprocess via subtraction of the π^- and π^+ inclusive yields.

In the limit $\theta^* \to 0$ for large x_R, $\hat{\sigma}(\pi^- u)/\hat{\sigma}(\pi^+ d) \to 1$. This is considerably less than the leading-twist factor of 4.

IV. NUMERICAL RESULTS

For $\pi^\pm p \to \gamma X$ the absolute inclusive yield of prompt photons predicted by Eq. (11) is presented in Figs. 3–5, and it is compared with the yield from the leading-twist subprocess $\bar{u}_\pi u_p \to \gamma g$ in $\pi^- p \to \gamma X$.

Simple structure functions are chosen so as not to obscure essential conclusions. In particular, $x u_p(x) \equiv (1-x)^3$ is normalized such that up quarks carry 25% of the proton momentum, and, for down quarks, $x d_p(x) = 0.5 x u_p(x)$. More detailed parametrizations including Q^2 evolution will not affect qualitative conslusions, but they may be warranted when future comparisons are made with relevant data. For the leading-twist subprocess $\bar{u}_\pi u_p \to \gamma g$ the QCD Born cross section is

$$\frac{1}{\pi}\frac{d\sigma_{\text{LT}}}{d\hat{t}} = D_{\text{LT}}\frac{1}{\hat{s}^2}\left[\frac{\hat{t}}{\hat{u}} + \frac{\hat{u}}{\hat{t}}\right] , \tag{17}$$

where $\hat{t}$ is the momentum transfer between the incident $\bar{u}_\pi$ and the final γ, $\hat{s} = x_1 x_2 s$, and $D_{\text{LT}} = \frac{8}{9}\alpha_{\text{EM}}\alpha_s e_u^2$, with $e_u = \frac{2}{3}$. The leading-twist inclusive yield is obtained from the convolution

$$\frac{E\, d\sigma_{\text{LT}}}{d^3p}(\pi^- p \to \gamma X) = \int_0^1 dx_1 \int_0^1 dx_2 \bar{u}_\pi(x_1) u_p(x_2) \frac{\hat{s} d\sigma_{\text{LT}}}{\pi d\hat{t}}(\bar{u}_\pi u_N \to \gamma g)\delta(\hat{s}+\hat{t}+\hat{u}) . \tag{18}$$

The quark structure function of the pion is chosen to have the simple behavior $x_1 \bar{u}_\pi(x_1) = 0.4(1-x_1)$, normalized such that the $\bar{u}$ quark in the π^- carries 20% of the pion's momentum. This simple linear form agrees with naive counting rules[10] and with data.[11] The use of a quadratic form, $x\bar{u}_\pi(x) \propto (1-x)^2$, having somewhat more theoretical justification,[2] would reduce the size of the predicted leading-twist yield. The leading-twist yield shown in Fig. 3(b) is in excellent agreement with other estimates.[12]

In the comparison of leading-twist and high-twist yields, any sensitivity to the choice of $u_p(x)$ is reduced since the same function enters both predictions. The leading-twist and high-twist yields are also both linearly proportional to α_s; their ratio is therefore independent of the choice made. The constant value $\alpha_s = 0.3$ is used here.

Other leading-twist subprocesses contribute to $\pi^- p \to \gamma X$, such as the three gluon Compton reactions $g_\pi q_p \to \gamma q$, $\bar{q}_\pi g_p \to \gamma \bar{q}$, and $q_\pi g_p \to \gamma q$, and the nucleon sea annihilation reaction $q_\pi \bar{q}_p \to \gamma g$. However, in $\pi^- p \to \gamma X$ the dominant leading-twist subprocess at large x_T and/or forward angles is $\bar{u}_\pi u_p \to \gamma g$. Large x_T and/or forward angles is precisely the kinematic region in which the high-twist contributions studied here should be most important. Therefore, it should suffice to limit our comparison to the results of $\bar{u}_\pi u_p \to \gamma g$, and to focus attention on the differences in x_T and p_T variations, as well as on beam-dependent charge ratios.

A. Cross sections

A first observation is that the predicted yields in Figs. 3–5 are small. For values of $p_T \gtrsim 4.5$ GeV/c, where the experimental[13] prompt γ/π^0 ratio is distinguishable from background, the high-twist process provides inclusive yields in the picobarn (10^{-36} cm^2) range for $p_{\text{lab}} \gtrsim 200$ GeV/c. Prompt photon experiments[13] are now sensitive to cross sections more than an order of magnitude below this level. Second, both in absolute terms

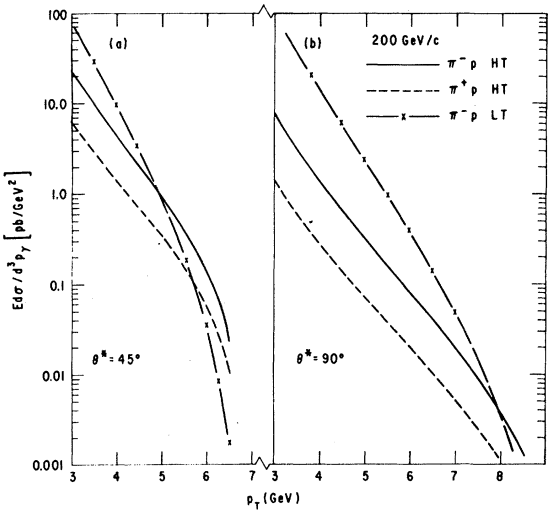

FIG. 3. Transverse-momentum dependence of the predicted inclusive prompt photon yield $E\,d\sigma/d^3p$ for $\pi^{\pm}p\to\gamma X$ at $\sqrt{s}=20$ GeV and at center-of-mass photon angles (a) $\theta^*=45°$, and (b) $\theta^*=90°$, measured with respect to the incident pion direction. Shown are the high-twist yields for $\pi^{\pm}p\to\gamma X$ obtained from the subprocess $\pi q\to\gamma q$, and, for comparison, the leading-twist yield in $\pi^- p\to\gamma X$, only, from the subprocess $\bar{u}_\pi u_p\to\gamma g$. For $\pi^+ p\to\gamma X$, the leading-twist yield from $\bar{d}_\pi d_p\to\gamma g$ is $\frac{1}{8}$ that shown for $\pi^- p\to\gamma X$.

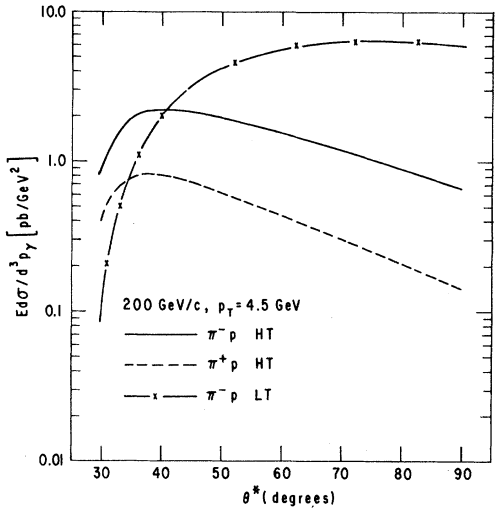

FIG. 5. Dependence of the predicted prompt photon yields on the center-of-mass scattering angle θ^* at $\sqrt{s}=20$ GeV and $p_T=4.5$ GeV.

and relative to the leading-twist contribution, the high-twist yield is greatest at forward c.m. angles. This point is illustrated in Fig. 5. The prospects for isolating the high-twist signal would seem best at $\theta^*<45°$. The expectations presented in Fig. 5 may be reexpressed in terms of rapidity y. For massless particles, including photons, $y=\frac{1}{2}\ln[(1+\cos\theta^*)/(1-\cos\theta^*)]$. The angle $\theta^*=40°$ corresponds to $y\simeq 1$.

Third, in $\pi^- p\to\gamma X$, even at $x_F=0$, and in the interesting range of $p_T\gtrsim 4.5$ GeV, the yield from the special high-twist process studied here is seldom significantly less than 10% of the yield from the leading-twist subprocess $\bar{u}_\pi u_p\to\gamma g$. This leading-twist subprocess accounts, in turn, for at least one-half of the estimated full inclusive yield[12] in $\pi^- p\to\gamma X$. Therefore, as long as a clean prompt photon signal is detected, it should be possible to isolate the high-twist contribution by exploiting its unique two-body kinematics and its characteristic

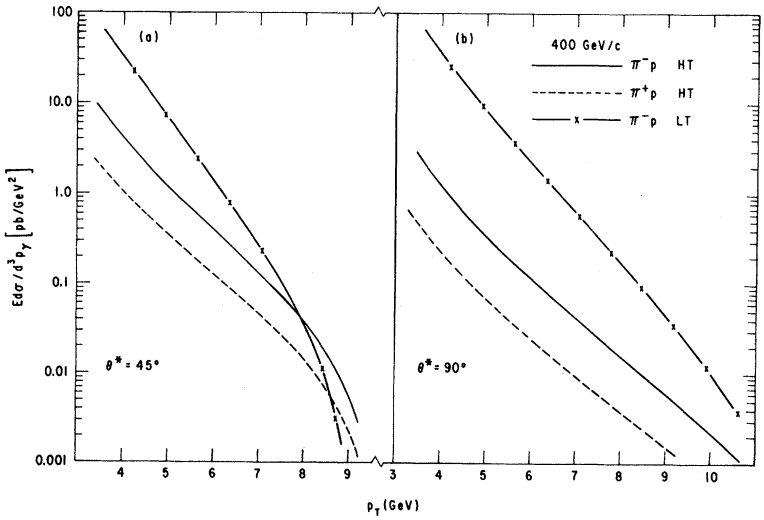

FIG. 4. As in Fig. 3, but for incident-pion laboratory momentum of 400 GeV/c.

topological property, the absence of a stream of spectator particles along the beam direction. Experimental apparatus with broad angular acceptance for charged hadrons and with fine segmentation is required to establish these features of the event structure.

B. Kinematic constraints

For the specific high-twist process considered here, whatever the γ production angle, conservation of energy and momentum require ($s \gg m_N{}^2$)

$$p_T^{\gamma}+p_T^{\text{jet}}=0 , \tag{19a}$$

$$(E+p_L)^{\gamma}+(E+p_L)^{\text{jet}}=(E+p_L)^{\pi} . \tag{19b}$$

Once p_T and the longitudinal momentum p_L are determined for the prompt γ, those of the recoil quark jet are fixed. Since the entire four-momentum of the incident pion in Fig. 1(a) is delivered to the QCD subprocess, there is no smearing of the jet kinematics associated with a spread of the incident hadron constituent longitudinal momentum. Smearing associated with intrinsic transverse momentum of the initial constituents is also reduced since only one initial constituent is present. By contrast, for the leading-twist process sketched in Fig. 1(b), a beam of spectator particles accounts for part of the initial pion's momentum, and Eq. (19b) is replaced by

$$(E=p_L)^{\gamma}+(E+p_L)^{\text{jet}}=x_1(E+p_L)^{\pi} , \tag{20}$$

with variable x_1.

In terms of light-cone momentum fractions defined as

$$\omega_i=(E^i+p_L^i)/(E^{\pi}+p_L^{\pi}) , \tag{21}$$

the high-twist events of interest are those for which $\omega_{\gamma}+\omega_{\text{jet}}\simeq 1$. Because ω_{jet} is the sum of the individual ω_k for each hadron component in the jet, the events of interest may also be defined as those for which $\omega_{\gamma}+\sum\omega_k=1$.

The high-twist signal should be isolated if a veto is imposed to reject events with hadrons emerging along the beam direction, and/or kinematic restrictions are imposed on the jet of hadrons which recoil at large p_T against the prompt photon.

C. Charge ratios

Remarks were made in Sec. III concerning the variation of the high-twist cross section with the charge of the incident π beam. The comparisons presented in Figs. 3(b) and 4(b) indicate that at $x_F=0$, $\sigma(\pi^+p\to\gamma X)\simeq\frac{1}{4}\sigma(\pi^-p\to\gamma X)$ over most of the interesting range of p_T. One half of this effect is due to the initial structure functions which are related by $d_{p(x)}=\frac{1}{2}u_p(x)$. At more forward angles, as shown in Figs. 3(a) and 4(a), the yields are related very approximately by $\sigma(\pi^+p\to\gamma X)\simeq\frac{1}{3}\sigma(\pi^-p\to\gamma X)$.

At the leading-twist level, the contribution from the subprocess $\bar{q}_{\pi}q_p\to\gamma g$ provides a simple relationship valid for all x_T and x_F: $\sigma_{\text{LT}}(\pi^+p\to\gamma X)=\frac{1}{8}\sigma_{\text{LT}}(\pi^-p\to\gamma X)$. Consequently, in $\pi^+p\to\gamma X$, the high twist subprocess plays a relatively more significant role when compared with the leading-twist subprocess $\bar{d}_{\pi}d_p\to\gamma g$. At $x_F=0$, the higher-twist term is always a significant "background." At $\theta^*=45°$, the π^+p high-twist yield *exceeds* the leading-twist yield for $p_T>4$ GeV at $p_{\text{lab}}=200$ GeV/c, and for $p_T>6.5$ GeV at $p_{\text{lab}}=400$ GeV/c.

When only the leading-twist subprocesses are important, an appropriate subtraction of the $\pi^-p\to\gamma X$ and $\pi^+p\to\gamma X$ inclusive yields results in cancellation of the gluon Compton processes, and a sample of annihilation events is left, produced by $\bar{q}q\to\gamma g$. The interpretation of this difference is cleanest when the subtraction is made of inclusive yields produced from an isoscalar target, such as C. It has been proposed to use the difference of yields to extract the x dependence of the quark structure function of the pion. In the difference, the p_T of the prompt photon is balanced by that of a gluon jet. In those regions of phase space in which the high-twist yield is significant, the difference of the yields from $\pi^-p\to\gamma X$ and $\pi^+p\to\gamma X$ (or of π^-C and π^+C) no longer isolates the annihilation subprocess, and, in particular, the difference does not leave a sample in which gluon jets dominate in the final-state recoil spectrum.

In π^-p interactions, the special high-twist process discussed in this paper specifies that a d quark recoils against the high-p_T prompt photon. If the high-twist sample is isolated in π^-p collisions according to the kinematic procedure discussed above, the data would provide a clean source of d quarks for fragmentation studies.

V. CONCLUDING REMARKS

In this paper, predictions are presented for the inclusive prompt-photon yield associated with a specific high-twist subprocess. The yield is nor-

malized absolutely in terms of the electromagnetic form factor of the pion, $F_\pi(Q^2)$. In $\pi^\pm N \to \gamma X$, the QCD subprocess involves a pointlike short-distance coupling of the *pion*. The observation of the predicted class of events would provide a significant verification of the applicability of the Fock-state decomposition of the pion wave function into color singlet $|q\bar{q}\rangle$ and higher components. High-p_T prompt photon events without hadron energy along the beam axis direction measure the amplitude associated with this $|q\bar{q}\rangle$ component. They comprise an event topology which probes the joint probability for finding both a q and a $\bar{q}$ in the beam, and only a q and $\bar{q}$. Events with no hadron energy radiated along the beam axis direction are possible only because the initial state which participates in the hard scattering (here a pion) is a color singlet.[6]

The procedure employed in this paper to normalize the high-twist yield is essentially identical to that used by Farrar and Fox[14] who predict a very small rate for $\pi q \to \pi q$. Although rates computed here for $\pi^\pm N \to \gamma X$ are also small, they are a substantial fraction of the inclusive yield in the laboratory momentum range 200 to 400 GeV/c, and they should be observable. It should be noted, moreover, that the particular high-twist subprocess studied in this paper provides a lower limit on the total p_T^{-6} contribution to $\pi^\pm N \to \gamma X$. Additional high-twist contributions are associated with other pion Fock-state components such as $|q\bar{q}g\rangle$ and $|q\bar{q}q\bar{q}\rangle$. In the decomposition of the pion state vector, it is estimated[15] that the probability attributed to the $|q\bar{q}\rangle$ component is roughly 25%.

Correspondingly, it is not unreasonable to suppose that the net high-twist contribution would be a factor of 4 greater than indicated in Figs. 3–5. Other high-twist subprocesses are associated with the nucleon target, such as $\bar{u}_\pi + (uu)_N \to \gamma u$, and with coherent effects in the final state, including $\bar{q}q \to \gamma\pi$. Most of these are more difficult to normalize than the special process treated in this paper, and they are not endowed with characteristic topological and kinematic properties. In an effort to isolate experimentally and to study a high-twist contribution with well defined properties, it would seem best to focus on the specific process discussed in this paper.

ACKNOWLEDGMENT

I am pleased to acknowledge valuable conversations with S. J. Brodsky. This work was performed under the auspices of the United States Department of Energy.

APPENDIX: $\bar{q}q \to \pi\gamma$

The expressions developed in Sec. II may be applied directly to derive predictions for the high-twist subprocess $\bar{q}q \to \gamma\pi$, obtained from $\pi q \to \gamma q$ via crossing. We redefine $\hat{s} = (p_\pi + p_\gamma)^2$, and $\hat{t} = (p_\gamma - p_{\bar{q}})^2$. The absolute square of $M(\hat{s},\hat{t})$, summed over final spins and colors, and averaged over initial spins and colors becomes

$$\frac{1}{36}\sum_{\substack{\text{colors,}\\ \text{spins}}} |M(\hat{s},\hat{t})|^2 = \frac{8}{81} e^2 g^4 \left[\frac{1}{\hat{u}^2} + \frac{1}{\hat{t}^2}\right] \frac{(e_2\hat{t} + e_1\hat{u})^2}{\hat{s}} \left| \int_0^1 \frac{\phi_\pi(z,Q)dz}{z(1-z)} \right|^2 . \tag{A1}$$

The differential cross section for $\bar{q}q \to \gamma\pi$ is

$$\frac{1}{\pi}\frac{d\sigma_{\rm HT}}{d\hat{t}} = \frac{2}{27}\alpha_{\rm EM}\alpha_s F_\pi(\hat{s}) \left[\frac{1}{\hat{u}^2} + \frac{1}{\hat{t}^2}\right] \frac{(e_2\hat{t} + e_1\hat{u})^2}{\hat{s}^2} . \tag{A.2}$$

Equation (A2) may be compared with the cross section for the leading-twist subprocess $\bar{q}q \to \gamma g$, Eq. (19). It is easy to show that

$$\frac{1}{\pi}\frac{d\sigma_{\rm HT}}{d\hat{t}} = \frac{1}{\pi}\frac{d\sigma_{\rm LT}^{(i)}}{d\hat{t}} \frac{F_\pi(\hat{s})(e_2\hat{t} + e_1\hat{u})^2}{12 e_i^2 \hat{t}\hat{u}} \tag{A3}$$

for $\bar{u}_\pi d_N \to \gamma\pi^-$, $e_1 = \frac{2}{3}$, and $e_2 = -\frac{1}{3}$, whereas for $\bar{d}_\pi u_N \to \gamma\pi^+$, $e_1 = -\frac{1}{3}$ and $e_2 = \frac{2}{3}$.

In events produced by quark-antiquark annihilation, the high-twist subprocess $\bar{q}q \to \gamma\pi^\mp$ provides a "prompt" charged-pion background to the gluon jets generated by the leading-twist process $\bar{q}q \to \gamma g$. A significant high-twist contribution would confuse the analysis of gluon fragmentation.

[1]The analyses by F. Eisele, CERN-Dortmund-Heidelberg-Saclay Collaboration and by M. Leenen of the European Muon Collaboration are discussed in recent reviews by C. Matteuzzi, in *Particles and Fields—1981: Testing the Standard Model,* proceedings of the Meetings of the Division of Particles and Fields of the APS, Santa Cruz, California, edited by C. A. Heusch and W. T. Kirk (AIP, New York, 1982) and by J. Drees, in *Proceedings of the 1981 International Symposium on Lepton and Photon Interactions at High Energy, Bonn,* edited by W. Pfeil (Universität Bonn, Bonn, 1981).

[2]E. L. Berger and S. J. Brodsky, Phys. Rev. Lett. 42, 940 (1979). See also Z. F. Ezawa, Nuovo Cimento 23A, 271 (1974) and G. R. Farrar and D. R. Jackson, Phys. Rev. Lett. 35, 1416 (1975).

[3]K. J. Anderson *et al.,* Phys. Rev. Lett. 43, 1219 (1979). See, however, J. Badier *et al.,* CERN Report No. CERN-EP/81-17, 1981 (unpublished).

[4]E. L. Berger, Phys. Lett. 89B, 241 (1980), and Z. Phys. C 4, 289 (1980).

[5]M. Haguenauer *et al.,* Phys. Lett. 100B, 185 (1981). See also the review by N. Schmitz, in *Proceedings of the 1981 International Symposium on Lepton and Photon Interactions at High Energies, Bonn* (Ref. 1).

[6]E. L. Berger and S. J. Brodsky, Phys. Rev. D 24, 2428 (1981). See also E. L. Berger, T. Gottschalk, and D. Sivers, *ibid.* 23, 99 (1981); D. Jones and R. Ruckl, Phys. Rev. D 20, 232 (1979).

[7]Photoproduction of high-twist events is studied by J. Bagger and J. F. Gunion, Phys. Rev. D 25, 2287 (1982), and by S. Matsuda, Report No. KEK-TH 37 (unpublished).

[8]G. P. Lepage and S. J. Brodsky, Phys. Rev. D. 22, 2157 (1980) and references therein. See also A. V. Efremov and A. V. Radyushkin, Phys. Lett. 94B, 245 (1980); A. Duncan and A. Mueller, Phys. Rev. D 21, 1636 (1980); and R. D. Field, R. Gupta, S. Otto, and L. Chang, Nucl. Phys. B186, 429 (1981).

[9]C. J. Bebek *et al.,* Phys. Rev. D 13, 25 (1976).

[10]S. J. Brodsky and G. R. Farrar, Phys. Rev. Lett. 31, 1153 (1973); R. Blankenbecler and S. J. Brodsky, Phys. Rev. D 10, 2973 (1974).

[11]C. B. Newman *et al.,* Phys. Rev. Lett. 42, 951 (1979); J. Badier *et al.,* Report No. CERN-EP/80-148, presented at the XXth International Conference on High Energy Physics, Madison, 1980 (unpublished).

[12]See Fig. 13b of F. Halzen and D. M. Scott, University of Wisconsin Report No. MAD/PH/21, 1981 (unpublished). However, these authors do not specify which structure functions were used.

[13]M. Diakonou *et al.,* Phys. Lett. 91B, 296 (1980); 91B, 301 (1980); C. Kourkoumelis *et al.,* Nucl. Phys. B179, 1 (1981); R. M. Baltrusaitis *et al.,* Phys. Lett. 88B, 372 (1979); A. Angelis *et al., ibid.* 98B, 115 (1981). For a recent review of the experiments, consult W. J. Willis, in *Proceedings of the 4th International Colloquium on Photon-Photon Interactions, Paris, 1981,* edited by Georges W. London (World Scientific, Singapore, 1981).

[14]G. Farrar and G. C. Fox, Nucl. Phys. B167, 205 (1980).

[15]S. J. Brodsky, T. Huang, and G. P. LePage, Report No. SLAC-Pub-2540, 1980 (unpublished).